

## Observation of Soliton Tunneling Phenomena and Soliton Ejection

Assaf Barak,<sup>1</sup> Or Peleg,<sup>1</sup> Chris Stucchio,<sup>2</sup> Avy Soffer,<sup>3</sup> and Mordechai Segev<sup>1</sup>

<sup>1</sup>*Physics Department, Technion - Israel Institute of Technology, Haifa 32000, Israel*

<sup>2</sup>*Courant Institute of Mathematical Sciences, New York University, New York 10012, USA*

<sup>3</sup>*Department of Mathematics, Rutgers University, New Brunswick, New Jersey 08903, USA*

(Received 21 January 2008; published 17 April 2008)

We study, theoretically and experimentally, the nonlinear dynamics of a wave packet launched inside a trap potential. Increasing the power of the wave packet transforms its dynamics from linear tunneling through a potential barrier, to soliton tunneling, and eventually, above a well-defined threshold, to the ejection of a soliton from the potential trap.

DOI: [10.1103/PhysRevLett.100.153901](https://doi.org/10.1103/PhysRevLett.100.153901)

PACS numbers: 42.65.Tg, 03.75.Lm

Tunneling is one of the most characteristic features of wave dynamics, manifesting itself in fascinating ways, from tunneling of charge-carriers [1], superconducting [2,3] and superfluid states [4], to tunneling of matter waves [5,6], and even quantum phase transitions [7], and Josephson effects in BEC [8]. In optics, tunneling has made its way into commercial devices, such as the directional coupler [9]. Solitons, on the other hand, are highly nonlinear creatures, whose entire existence stems from nonlinear waves. Although these two phenomena seem completely unrelated, recent theory papers [10,11] suggested the possibility of matter-wave (BEC) solitons tunneling through a potential barrier. These predictions are conceptually related to propositions made a decade ago, in the context of temporal solitons in optical fibers, suggesting that solitons can tunnel in the temporal domain through a longitudinal junction [12], and in the frequency domain across a forbidden normal-dispersion barrier [13]. The recent prediction of matter-wave soliton tunneling [10,11] has direct implications for optical spatial solitons. Thus far, however, soliton tunneling has never been studied experimentally, in any physical system.

Here, we demonstrate soliton transport phenomena through a potential barrier. We study the nonlinear dynamics of an optical beam launched into a trap potential. At low power levels, the light tunnels linearly out of the trap. As we increase the initial power level, the tunneled power accumulates and forms a bright soliton, while most of the initial power remains inside the potential trap. When the initial power is further increased, the beam overcomes the potential barrier, and a narrow soliton is ejected out of the trap, carrying within most of the power. To our knowledge, this is the first experimental observation of soliton tunneling and of soliton ejection, in any system in nature.

To conform with our experiments, we analyze the problem in the framework of the photorefractive screening nonlinearity [14], where we employ the optical induction technique to make the potential trap [15,16]. However, the ideas involved are general, irrespective on how the potential is made (or induced), and irrespective on whether the nonlinearity is Kerr type [10,11] or saturable (e.g., the

photorefractive screening nonlinearity [14], or the nonlinearity in homogeneously-broadened two-level systems [9]). The problem is formulated by the (2+1)D NLSE with a saturable nonlinearity [14], describing the propagation of a paraxial monochromatic beam launched in a trap potential,

$$2ik_0 \frac{\partial \psi}{\partial z} + \nabla_{\perp}^2 \psi - 2k_0^2 \frac{\Delta n_0/n_0}{1 + I_{\text{POT}} + |\psi|^2} \psi = 0. \quad (1)$$

Here,  $\psi$  is the envelope of the propagating field, and  $I_{\text{POT}}$  is the intensity that induces the trap potential ( $|\psi|^2$  and  $I_{\text{POT}}$  are normalized to the background illumination),  $k_0 = \frac{2\pi n_0}{\lambda}$  is the wave number,  $n_0$  is the linear refractive index in the medium, and  $\lambda$  is the vacuum wavelength. Also,  $\Delta n_0 = \frac{1}{2} n_0^3 r_{33} E$  is the nonlinear refractive-index change, where  $r_{33}$  is the relevant electro-optic coefficient, and  $E$  is the applied field. We use  $\lambda = 488$  nm,  $n_0 = 2.35$ ,  $r_{33} = 1200$  pm V<sup>-1</sup>, and  $E = 200$  V cm<sup>-1</sup>, as in our experiments.

We analyze the nonlinear dynamics of a wave packet launched inside the trap by simulating Eq. (1). We launch a 35  $\mu\text{m}$  FWHM Gaussian beam, into the trap, as shown in Fig. 1(a). When the barrier is much wider than the width of the beam, there is almost no power transport through the barrier: the beam oscillates inside the trap for many periods [Fig. 1(b)]. When we decrease the width of the barrier to be comparable to the width of the beam, power starts to tunnel linearly across the barrier, and the power remaining in the trap decays exponentially with the propagation distance [Fig. 1(c)]. The light that has tunneled out of the trap propagates mostly linearly, forming a broad nonlocalized wave. As we increase the power of the launched beam, the tunneled power accumulates at the external margins of the barrier and forms a soliton (of 15  $\mu\text{m}$  FWHM) that continues to propagate without broadening, over many diffraction lengths [Fig. 1(d)]. Under these conditions, most of the initial power remains inside the trap. When we further increase the initial power, the index change induced by the beam is high enough to overcome the potential barrier, and the transport out of the trap is no longer through tunneling. Rather, the beam is attracted towards the region

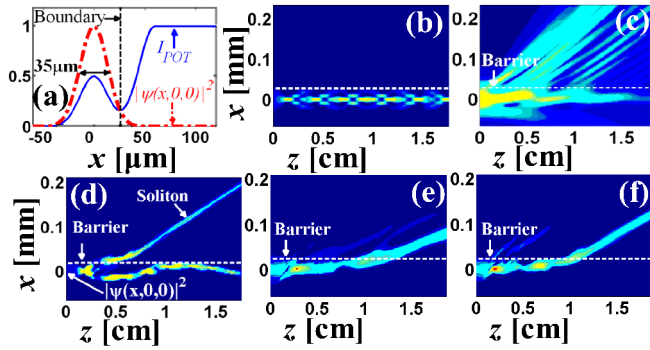


FIG. 1 (color online). Cross sections of (2+1)D beam propagation under different initial conditions. (a) The intensity profile of the initial wave function (dotted red), and of the light inducing the trap potential. (b) Propagation of the beam in the presence of a wide barrier. (c) Linear tunneling of low-intensity beam [ $\psi(0, 0, 0) = 0.3$ ]. (d) Soliton tunneling from the potential trap [ $\psi(0, 0, 0) = 1.35$ ]. (e), (f) Soliton ejection at increasingly higher input intensities  $\psi(0, 0, 0) = 2$ ,  $\psi(0, 0, 0) = 3$ , respectively.

of higher refractive index, and a soliton is ejected from the trap [Fig. 1(e)]. The ejected soliton carries more than 90% of the power contained in the initial beam, and it has a 20  $\mu\text{m}$  FWHM. We find that the ejection process exhibits a sharp intensity threshold that clearly distinguishes between two generically different regimes: linear tunneling of a soliton and the ejection of a soliton. The intensity threshold and the dynamics of the soliton at the vicinity of this threshold will be analyzed in details later on. Finally, when we increase the power even further, it is easier for the beam to overcome the barrier, and the soliton ejection process occurs earlier [Fig. 1(f)].

Experimentally, the formation of the trap relies on the optical induction technique, in which a refractive-index profile is induced in a nonlinear medium [15,16]. We use a 1 cm long SBN:75 crystal, with  $r_{33} = 1200 \text{ pm V}^{-1}$ . The refractive-index profile (the potential trap) is generated by the intensity superposition of two mutually uncorrelated ordinarily polarized beams. The first induction beam is of 35  $\mu\text{m}$  FWHM and is used to induce the trap. This width has negligible diffraction over the 1 cm propagation distance, hence the induced trap is effectively propagation-invariant. By changing the width of this first induction beam and its intensity, we control the trap width and its depth. The second induction beam creates the external region outside the trap, to which the soliton is ejected. This beam has a step-function structure, generated by a sharp knife-edge, cutting half of a broad beam (0.5 cm FWHM). The step-beam is passed through a spatial filter, facilitating control over the slope of the step, while the intensity of this beam controls the strength of the index change in the external region. We set the step to increase from 0% to 100% within  $\sim 40 \mu\text{m}$ , making its diffraction-broadening negligible. Hence, the induced potential is propagation-invariant. Figures 2(a) and 2(b) show the in-

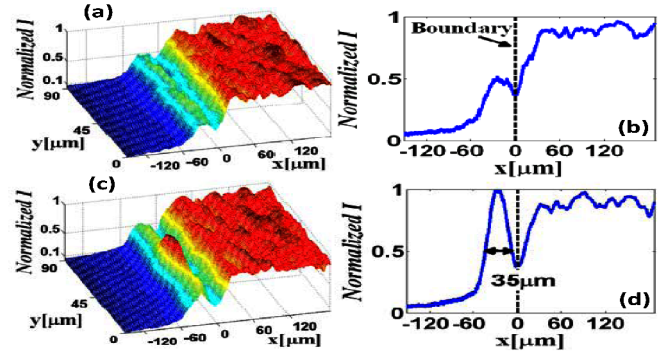


FIG. 2 (color online). Experimental intensity photographs at the input plane of the sample. (a), (b) The intensity profile inducing the trap potential and its cross section. (c), (d) Total intensity at the input plane: sum of the intensities of the (ordinarily polarized) beam inducing the trap potential and of the (extraordinarily polarized) launched beam, for  $|\psi(0, 0, 0)|^2 \approx 4$ , and its cross section. The total intensity reflects the overall potential: linear + the nonlinear part induced by the launched beam.

tensity profile of the beams inducing the overall potential at the input face of the crystal.

After forming the trap potential, we launch a 35  $\mu\text{m}$  FWHM extraordinarily polarized beam at the center of the trap, as shown in Figs. 2(c) and 2(d). When no external field is applied, there are no noticeable nonlinear effects: the beam diffracts (broadens) linearly, while propagating on-axis in the homogenous medium, exiting the sample with  $\sim 45 \mu\text{m}$  FWHM [Fig. 3(a)]. Next, we apply a field of 1000 V/cm, and create a wide barrier, separating the “potential well” and the “external region” by a barrier of 120  $\mu\text{m}$ . Under the action of nonlinearity, the beam narrows, while propagating on-axis inside the trap without changing its trajectory [Fig. 3(b)]. We then reduce the width of the barrier to be on the order of the width of the beam, but keep the power of the launched beam low. Under these conditions, power starts to linearly tunnel out of the trap [Fig. 3(c)]. However, a bright soliton does not form, since the tunneled power and the tunneling rate are not high enough to support a soliton. When we increase the power of the launched beam, the tunneling rate increases, and the beam that has tunneled out of the trap has sufficient power to form a narrow (13  $\mu\text{m}$  FWHM) soliton outside the trap. Consequently, the output intensity structure in this case consists of two well-separated narrow, self-localized, beams [Fig. 3(d)]. The beam with the higher power still resides inside the trap and forms a soliton there. Nevertheless, the beam that has tunneled out of the trap, albeit having a lower power, forms a soliton right outside the barrier. Next, we further increase the power of the launched beam, and now the whole power that was initially launched into the trap crosses the barrier. This indicates that the beam has induced an index change that overcomes the potential barrier, hence a soliton is ejected out of the

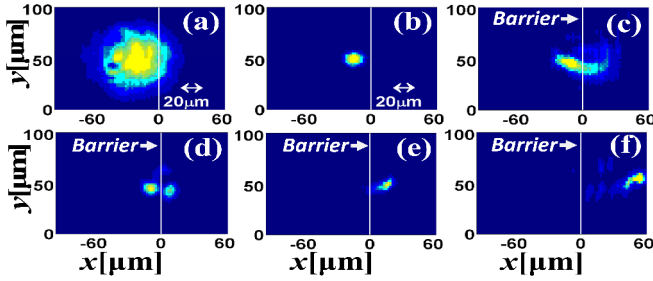


FIG. 3 (color online). Experimental photographs of the intensity structure at the output face of the sample, under various conditions. The vertical line marks the maxima of the external barrier. (a) Linear propagation, displaying on-axis propagation in a homogeneous system. (b) Nonlinear propagation of the beam when the barrier is too wide to observe tunneling effects; the beam forms a soliton propagating on-axis within the trap. (c) Linear tunneling of a low power beam through a narrow barrier [ $\psi(0, 0, 0) \approx 0.3$ ]. (d) Soliton tunneling: the power tunneled out of the trap forms a soliton moving away from the trap [ $\psi(0, 0, 0) \approx 1$ ]. (e, f) Soliton ejection at increasing power levels [ $\psi(0, 0, 0) \approx 2$ ,  $\psi(0, 0, 0) \approx 8$ , respectively]. The higher the initial power, the earlier the soliton ejection process occurs.

trap. Finally, as we further increase the input power, the ejected soliton exits the sample further away from the barrier [Figs. 3(e) and 3(f)], displaying a maximal deflection of  $80 \mu\text{m}$  away from the trap center [Fig. 3(f)].

We find experimentally and numerically that the process of soliton transport through the barrier displays two distinct regimes, separated by a sharp intensity threshold. When the intensity of the soliton is below threshold [ $|\psi(0, 0, 0)|^2 < |\psi_{\text{TH}}|^2$ ], most of the power ( $> 70\%$ ) stays in the trap, and soliton ejection does not occur. However, when the initial intensity is above threshold [ $|\psi(0, 0, 0)|^2 > |\psi_{\text{TH}}|^2$ ], a narrow soliton is ejected from the trap, carrying most of the initial power. This threshold arises from the nonlinear interaction between the soliton and the external potential: the soliton induces a change in the initial potential, which “liberates” the soliton from the trap. One can identify the threshold quantitatively, assuming that the external potential varies slowly, such that the soliton does not change its shape until it is ejected. Hence, we may analyze the interaction between the soliton and the total potential (as a fixed term and a nonlinear term) at the vicinity of the threshold intensity, by an effective particle model. This model describes the motion of  $\bar{x}$ , the average position of the soliton in the  $x$  direction, by [17]

$$\frac{d^2\bar{x}}{dz^2} = 2p^{-1} \int_{-\infty}^{\infty} \int_{-\infty}^{\infty} \frac{\partial F}{\partial x} \psi \psi^* dx dy, \quad (2)$$

where  $p = \int_{-\infty}^{\infty} \int_{-\infty}^{\infty} \psi \psi^* dx dy$  is the normalized soliton power, and  $F$  represents the total refractive index change (linear + nonlinear). Here,  $F$  arises from the saturable nonlinearity, yielding  $F = \frac{-\Delta n_0 / (2n_0)}{1 + I_{\text{pot}} + |\psi|^2}$ , which depends both on the soliton shape, and on the external (linear)

potential. Similarly, the motion of  $\bar{y}$ , the average  $y$  position of the soliton, can be described. However, since  $F$  and  $\psi$  are symmetric with respect to  $y$ , no optical force is exerted on the beam in the  $y$  direction, and the dynamics of the beam is solely in  $x$ . The expression on the right-hand side of Eq. (2) represents the effective force acting on the equivalent particle, which can be expressed as minus the gradient of an effective potential,  $\varphi(x)$ :

$$\frac{d^2\bar{x}}{dz^2} = -\frac{d\varphi(\bar{x})}{d\bar{x}}. \quad (3)$$

Equation (3) describes the motion of a particle under the influence of a nonlinear effective potential, which depends on the position of the particle. We find the threshold intensity, by calculating the effective potential for different soliton powers, as shown in Fig. 4(a). As in the experiments, we launch a Gaussian beam of an intensity value at the vicinity of the threshold, and simulate its dynamics [Figs. 4(b)–4(d)]. The Gaussian beam sheds some of its power to radiation (via tunneling through the barrier) while forming a soliton within the trap. The beam remaining in the trap behaves as if it is a soliton (albeit after a long propagation distance it will eventually tunnel out of the

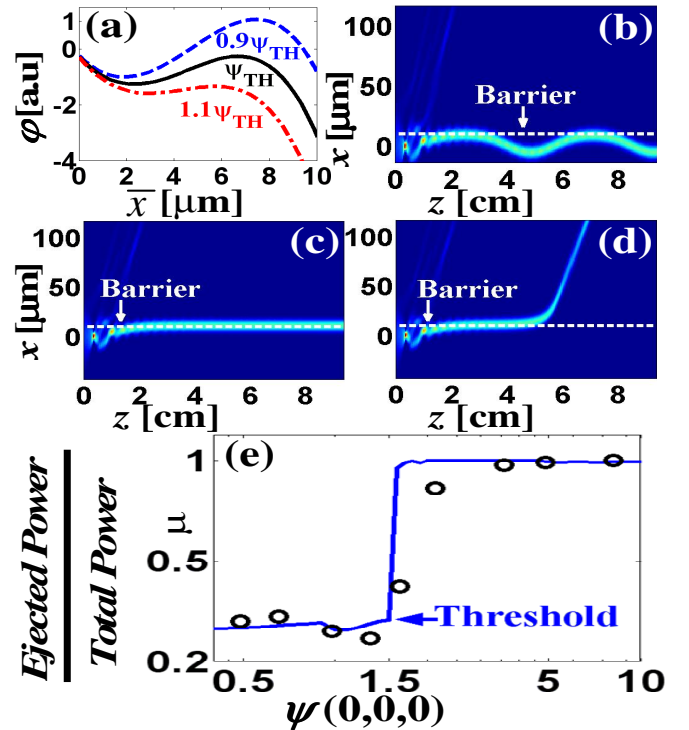


FIG. 4 (color online). (a) Effective induced potential for different values of  $\psi(0, 0, 0)$ . Simulated propagation of a beam launched inside a potential trap with (b)  $\psi(0, 0, 0) \approx 0.9\psi_{\text{TH}}$ , (c)  $\psi(0, 0, 0) \approx \psi_{\text{TH}}$ , (d)  $\psi(0, 0, 0) = 1.1\psi_{\text{TH}}$ . (e) Experimentally measured (black circles) and numerically calculated (smooth blue line) values of the power ejected from the trap (normalized by the total power) vs amplitude of the launched beam, for near-threshold values.

trap), and its intensity determines whether ejection occurs or not. Below threshold [blue-dashed line in Fig. 4(a)], the initial energy of the particle is lower than the potential barrier. This indicates that the soliton cannot pass the barrier, but instead it oscillates inside the trap, as shown in Fig. 4(b). Exactly at threshold, the initial energy of the particle is equal to the peak of the potential barrier [black-smooth line in Fig. 4(c)]. Under this condition, the particle does arrive to the peak of the barrier, but, since the equivalent force acting on it at that point is zero ( $\vec{\nabla}\varphi = 0$ ), it remains there indefinitely. This is equivalent to the soliton arriving at the peak of the potential barrier, yet never crossing it, but instead remaining at the barrier, and propagating on-axis as a surface wave at the barrier [Fig. 4(c)]. This surface wave is unstable, and will eventually divert from its course. Finally, as we increase the initial intensity to above the threshold, the peak of the potential barrier drops below the initial energy of the particle and the particle is free to pass the barrier [red-dotted-dashed line in Fig. 4(a)]. In this case, a soliton is ejected from the trap, as shown in Fig. 4(d). Note that in the ejection process, *all of the power launched into the trap is ejected*, and, consequently, the features of the ejected soliton (width, intensity) are predetermined, irrespective of the structure of the trap. The experimental results corroborate this intuitive theory. Figure 4(e) displays the experimentally measured (black circles) and numerically calculated (smooth blue line) power (normalized to the launched power) ejected from the trap vs peak amplitude of the launched beam, at the vicinity of the threshold. As in the theory, below threshold ( $\Psi_{\text{TH}} \approx 1.5$ ), most of the launched power remains inside the trap, whereas above threshold most of the launched power is ejected from the trap as a soliton.

The phenomenon of soliton ejection is worth further discussion. In the current study, the launched wave packet forms a soliton inside the trap, and above the threshold intensity it is ejected through the barrier. This process is inherently different from previous studies of “soliton emission”, which have been proposed [18,19] and demonstrated [20,21] in optical waveguides. Those previous studies on soliton emission refer to the generation of a soliton from a nonsoliton wave packet. As such, they are fundamentally different from the soliton ejection effects described here, which have never been addressed before.

In conclusion, we presented the first experimental study of soliton tunneling and soliton ejection through potential barriers. We have introduced a simple general method for identifying the threshold for soliton ejection. These ideas of soliton transport through potential barriers raise many new ideas in soliton physics. For example, it is possible to engineer a “soliton gun”, emitting a sequence of solitons through the barrier [10,18]. Likewise, it is possible to design a “soliton ejector”, where the ejection process is controlled either by the structure of the potential barrier, or in real time via interaction with another wave. The equivalence

between the spatial and temporal domains makes these results relevant for the studies of short pulses dynamics in waveguides, which leads to fascinating phenomena such as supercontinuum generation [22]. Another intriguing possibility has to do with “environment engineering.” Recent papers suggested altering linear tunneling effects (specifically, designing nonexponential tunneling) by modulating the coupling to continuum and engineering the potential of the “environment” outside the trap [23,24]. In this vein, it should be possible to engineer the nonlinear process of solitons tunneling through barriers and of soliton ejection, by properly designing the potential outside the trap. We emphasize that these results are general, and the ideas developed here can be implemented in other soliton-supporting systems beyond optics.

This work was supported by the Israeli Science Foundation.

- 
- [1] L. Esaki, Phys. Rev. **109**, 603 (1958); H. R. Zeller and I. Giaever, Phys. Rev. **181**, 789 (1969).
  - [2] B. D. Josephson, Phys. Lett. **1**, 251 (1962).
  - [3] P. W. Anderson and J. M. Rowell, Phys. Rev. Lett. **10**, 230 (1963).
  - [4] S. V. Pereverzev *et al.*, Nature (London) **388**, 449 (1997).
  - [5] B. P. Anderson and M. A. Kasevich, Science **282**, 1686 (1998).
  - [6] M. Albiez *et al.*, Phys. Rev. Lett. **95**, 010402 (2005).
  - [7] M. Greiner *et al.*, Nature (London) **415**, 39 (2002).
  - [8] S. Levy *et al.*, Nature (London) **449**, 579 (2007).
  - [9] A. Yariv, *Quantum Electronics*, (Wiley, New York, 1989), 3rd ed.
  - [10] M. I. Rodas-Verde, H. Michinel, and V. M. Pérez-García, Phys. Rev. Lett. **95**, 153903 (2005).
  - [11] G. Dekel *et al.*, Phys. Rev. A **75**, 043617 (2007).
  - [12] D. Anderson *et al.*, J. Opt. Soc. Am. B **11**, 2380 (1994).
  - [13] V. N. Serkin, V. A. Vysloukh, and J. R. Taylor, Electron. Lett. **29**, 12 (1993); B. Kibler *et al.*, Electron. Lett. **43**, 967 (2007).
  - [14] M. Segev *et al.*, Phys. Rev. Lett. **73**, 3211 (1994); M. Segev, M. F. Shih, and G. C. Valley, J. Opt. Soc. Am. B **13**, 706 (1996).
  - [15] N. K. Efremidis *et al.*, Phys. Rev. E **66**, 046602 (2002).
  - [16] J. W. Fleischer *et al.*, Nature (London) **422**, 147 (2003).
  - [17] A. B. Aceves, J. V. Moloney, and A. C. Newell, Phys. Rev. A **39**, 1809 (1989).
  - [18] E. M. Wright *et al.*, Phys. Rev. A **34**, 4442 (1986).
  - [19] M. A. Gubbels *et al.*, J. Opt. Soc. Am. B **4**, 1837 (1987).
  - [20] P. Dumais *et al.*, Opt. Lett. **25**, 1282 (2000).
  - [21] F. Baronio *et al.*, Opt. Lett. **28**, 2348 (2003).
  - [22] J. Herrmann *et al.*, Phys. Rev. Lett. **88**, 173901 (2002); J. M. Dudley, G. Genty, and S. Coen, Rev. Mod. Phys. **78**, 1135 (2006).
  - [23] A. G. Kofman and G. Kurizki, Phys. Rev. Lett. **87**, 270405 (2001).
  - [24] S. Longhi, Phys. Rev. Lett. **97**, 110402 (2006).